

# Activation and Fixation of Atmospheric CO<sub>2</sub> Through a 1,2,3-Triazole-based Mesoionic Carbene-Boron Adduct

Maren Neubrand<sup>#</sup>, Jessica Stubbe<sup>#</sup>, Richard Rudolf, Robert R. M. Walter, Maite Nöbller, Biprajit Sarkar\*

Dr. J. Stubbe, Dr. M. Nöbller, Prof. Dr. B. Sarkar

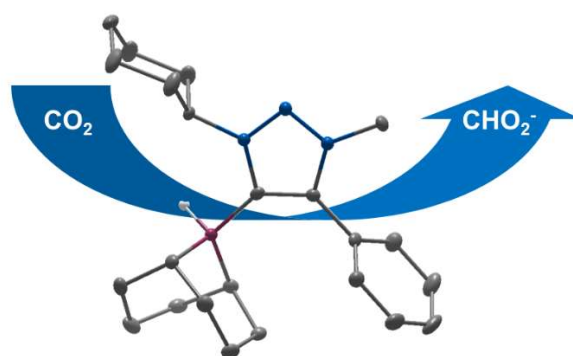
Institut für Chemie und Biochemie, Anorganische Chemie, Freie Universität Berlin,  
Fabeckstraße 34–36. 14195 Berlin, Germany

M. Neubrand, R. Rudolf, R. R. M. Walter, Prof. Dr. B. Sarkar

Institut für Anorganische Chemie, Universität Stuttgart, Pfaffenwaldring 44, 70569 Stuttgart, Germany

E-Mail: [biprajit.sarkar@iac.uni-stuttgart.de](mailto:biprajit.sarkar@iac.uni-stuttgart.de)

<sup>#</sup>Both authors contributed equally to this work.



## Abstract

Capturing atmospheric CO<sub>2</sub> and converting it to valuable chemicals are important goals in contemporary science. We present here a simple, transition metal-free triazolylidene-borane adduct that can capture atmospheric CO<sub>2</sub> and convert it to formate. Several key intermediates were isolated and characterized by a combination of multinuclear NMR spectroscopy, IR spectroscopy and single crystal X-ray diffraction. A first closed cycle for the conversion of CO<sub>2</sub> to formic acid by using the aforementioned triazolylidene-borane compound is presented as well.

## Introduction

Climate change is an undeniable fact and the escalating level of atmospheric carbon dioxide is one of the most pressing environmental concerns of our age. The environmental consequences are basis for political initiatives on a global scale, which are driven by the aim of reducing the emission of greenhouse gases, most notably carbon dioxide.<sup>[1]</sup> Technologies exist that are able to trap the CO<sub>2</sub> from the flue gas of major emitters, however, the price of carbon dioxide is too low to be a motivation for industrials to increase their efforts in recovering the greenhouse gas.<sup>[2]</sup> The utilization of CO<sub>2</sub> as a C<sub>1</sub> feedstock for the generation of industrially relevant chemicals is certainly an interesting different approach.<sup>[3]</sup> CO<sub>2</sub> is an attractive renewable C<sub>1</sub> source, which can lead to fuel-related products such as methane, methanol, and formic acid.<sup>[4]</sup> Those approaches would not only reduce the carbon dioxide emission through carbon capture, the costs of the sequestration could also be compensated by the production of chemicals which are in global demand.<sup>[5]</sup> Most of the liquid fuels used are based on fossil fuels, which again generate new CO<sub>2</sub> in the atmosphere. Indeed, by utilization of existing CO<sub>2</sub> for the generation of liquid fuels, the carbon footprint could be significantly reduced. Methanol is thereby one of the most promising energy vectors, since it could replace liquid fuels in modern technologies.<sup>[4]</sup>

In the past years, several reports based on the reduction of CO<sub>2</sub> through various transition metal compounds,<sup>[6-12]</sup> metal-free catalysts<sup>[13-18]</sup> or direct reduction with NaBH<sub>4</sub> without catalysts<sup>[19]</sup> have been published. But it is still a problem to capture the CO<sub>2</sub> present in the atmosphere, due to its low concentration, and furthermore, to reduce it to obtain fuels under ambient conditions. The first report on transition metal-free CO<sub>2</sub> capture from air, including the consecutive reduction of the CO<sub>2</sub> to produce a methanol precursor, which can be easily converted into methanol under ambient conditions, was made by the group of Mandal in 2019.<sup>[20]</sup> They reported an imidazole-based mesoionic carbene (Figure 1) supported 9-BBN adduct, which is able to perform the described conversion, including a thorough investigation of the mechanistic pathway. In recent years, the combination of a B-center together with carbenes or other main group components has turned out to be an attractive strategy for activating and converting inert bonds in small molecules.<sup>[21-28]</sup>

Since the first report on mesoionic carbenes (MIC) of the 1,2,3-triazol-5-ylidene (Figure 1) type more than 15 years back, the chemistry of this compound class has been dominated by transition metals.<sup>[29-32]</sup> prominent examples include applications in homogeneous catalysis, electrocatalysis, photochemistry/photophysics, and in the stabilization of unusual metal oxidation states.<sup>[29-35]</sup> In addition, a few reports have appeared either on the transformations of MICs into organic redox systems,<sup>[36]</sup> or on the combination of MICs with main group element fragments.<sup>[29, 37-39]</sup> In the following, we report the synthesis and characterization of a 1,2,3-triazol-5-ylidene-based MIC supported 9-BBN adduct. This MIC-borane adduct can capture atmospheric CO<sub>2</sub>, and convert it to formic acid. Investigations of a few key intermediates via multi nuclear NMR spectroscopy, IR spectroscopy and single crystal X-ray diffraction allows us to postulate a plausible reaction mechanism. Additionally, a first catalytic cycle for this process is presented as well.

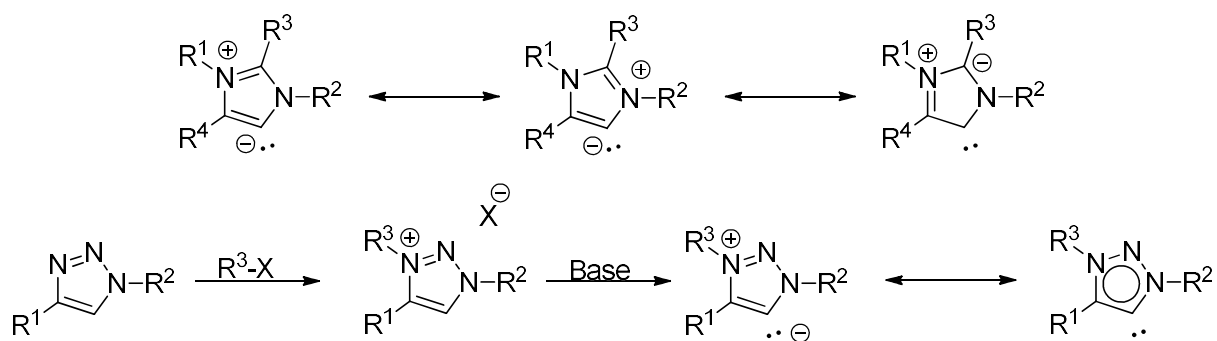
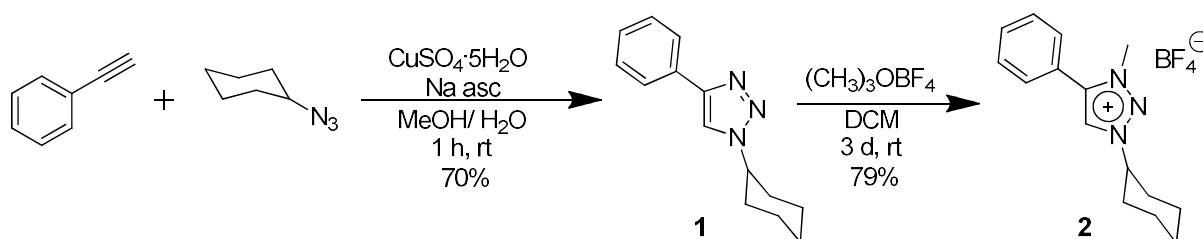


**Figure 1:** Resonance structures of a generic imidazole based MIC (top) and a generic triazole based MIC (with an exemplary resonance formula), obtained by alkylation of the triazole and deprotonation of the triazolium salt (bottom).

## Results and Discussion

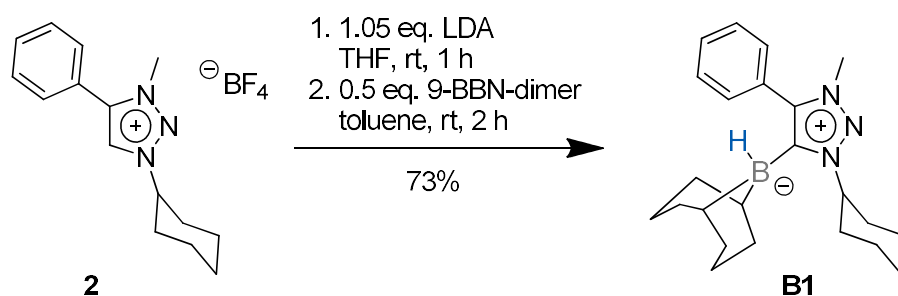
Our research started with the synthesis of the triazolium salt **2** as a precursor for the desired MIC-9-BBN adduct. **2** was generated through methylation of the 1,2,3-triazole **1** using Meerwein's reagent, and the triazole **1** itself was constructed by the cycloaddition of cyclohexyl azide and phenyl alkyne under standard click conditions (Scheme 1).

**Scheme 1.** Synthesis of the triazole **1** and the triazolium salt **2**.



With the aim of generating a MIC-9-BBN (9-BBN = (9-borabicyclo[3.3.1]nonane)) adduct, **2** was deprotonated with LDA at room temperature in the presence of the 9-BBN dimer (Scheme 2).

**Scheme 2.** Synthesis of the MIC-borane adduct **B1**.



The reaction progress was controlled *via* <sup>1</sup>H NMR spectroscopy, in which the disappearance of the triazolium-*H* signal at 8.58 ppm indicates the clean deprotonation of the former triazolium salt. The nucleophilic attack of the *in situ* generated 1,2,3-triazol-5-ylidene to the 9-BBN dimer led to the formation and isolation of the 1,2,3-triazol-5-ylidene-based MIC-9-BBN adduct **B1** in 73% yield. Single crystals could be obtained by the slow diffusion of *n*-hexane into a toluene solution of **B1** under inert conditions. **B1** displays a signal at -17.2 ppm in the <sup>11</sup>B spectrum. In the solid-state molecular structure of **B1**, the bond lengths within the triazolylidene moiety are in accordance with values previously reported in the literature (Figure 2).<sup>[30]</sup> The distance between the carbene C3 and the boron B1 is 1.634(2) Å and is in the same range as reported earlier for related compounds.<sup>[20]</sup>

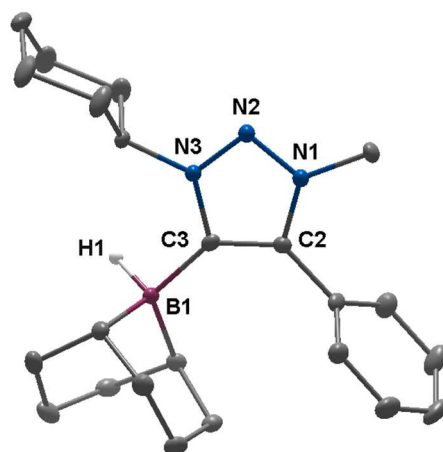


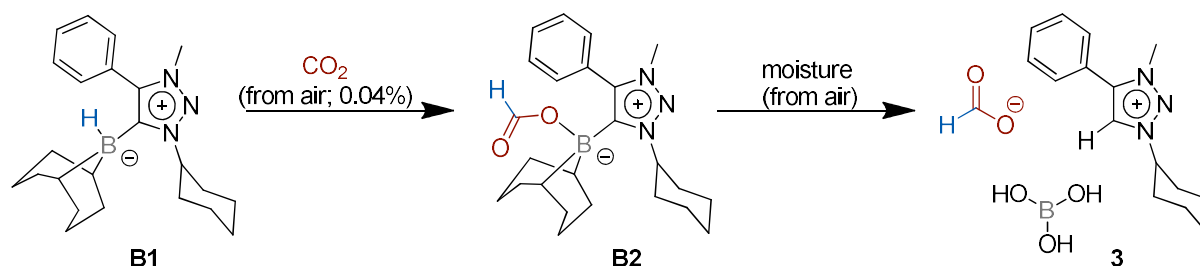
**Figure 2:** ORTEP representation of **B1**: ellipsoids drawn at 50% probability. Solvent molecules and H-atoms omitted for clarity. (For selected bond lengths and angles see supporting information Table S1).

The electrochemical properties of **B1** were investigated through cyclic voltammetric measurements (CV) in a MeCN/0.1 M NBu<sub>4</sub>PF<sub>6</sub> solution, (Figure S7). The CV shows a single reduction and two oxidation waves, which are all irreversible. The irreversibility is not influenced by increasing the scan rates of the measurements.

We were interested in the capability of **B1** in capturing CO<sub>2</sub> from air, therefore, a solution of **B1** was stirred in benzene under ambient air over night. The resulting <sup>1</sup>H NMR spectrum shows a crude reaction mixture, including the intact **B1**, and an additional product mixture, which includes the compounds **B2** and **3** (Scheme 3), analogue to the observations made by Mandal and co-workers.<sup>[17]</sup> In <sup>1</sup>H NMR spectra recorded in CD<sub>3</sub>CN, characteristic signals of all compounds can be found between 4.6 and 5.3 ppm, corresponding to the cyclohexyl-CH attached to the triazolium-unit. These signals are low-field shifted, due to the positive charge of the close triazolium-moiety and integrate to one proton. Considering these signals, a clear distinction of present species or at least the number of species in the reaction mixture can be made. The crude NMR (see supporting information, Figure S18) shows three of those characteristic multiplets, therefore corresponding to at least 3 different species in the mixture. The low field region of the spectra shows two sharp and one broadened singlet at 8.74, 8.62 and 8.26 ppm. In a mixture of **B2** and **3**, one would expect a signal caused by the attached formate in **B2**, two singlets corresponding to the formate anion and the newly formed triazolium-H in **3**. Crystallization attempts in an acetonitrile/diethyl ether mixture of the crude reaction mixture led to the formation of single crystals. Unfortunately, we were not able to collect structural data of the crystal of sufficient quality for the discussion of bond lengths and bond angles. However, the connectivity in the molecule is observed and presents one CO<sub>2</sub> molecule fixed as formate to the MIC-9-BBN adduct leading to the compound **B2**

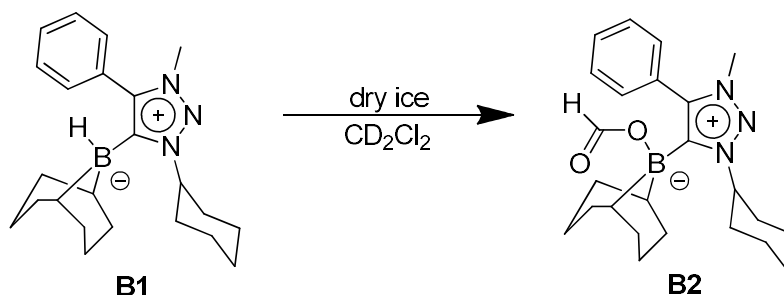
(Figure S4). These NMR and crystallographic results thus clearly show that the MIC-borane adduct **B1** can bind atmospheric CO<sub>2</sub> and convert it to formate. Unfortunately, the compounds **B2** and **3** generated through this method could not be separated and isolated in bulk. We therefore followed two alternative strategies to achieve a full characterization of the products, and to establish a first catalytic cycle for CO<sub>2</sub> reduction with respect to **B1**.

**Scheme 3:** Reaction of **B1** with atmospheric CO<sub>2</sub>.



The reaction of **B1** with dry ice as a CO<sub>2</sub> source led to the clean formation of **B2** (Scheme 4).

**Scheme 4.** Reaction of **B1** with dry ice for the formation of the formate complex **B2**.



The formation of **B2** was confirmed by several spectroscopic methods. In the <sup>1</sup>H NMR spectrum a new singlet appears at 8.27 ppm which can be assigned to the formate-proton (Figure 3). The signals obtained for **B2** match with those observed in the crude reaction mixture of **B1** with atmospheric CO<sub>2</sub> (Figure S18). In the <sup>11</sup>B NMR spectrum **B2** displays a singlet at -1.46 ppm which is a completely different chemical shift in comparison to **B1** (Figure 4). Additionally, in the <sup>1</sup>H coupled <sup>11</sup>B spectrum, **B1** shows a doublet, whereas **B2** displays only a singlet indicating the loss of the B-H proton. Furthermore, a strong peak is observed at 1666 cm<sup>-1</sup> in the IR spectrum of **B2** (Figure 5). This peak can be assigned to the carbonyl group of the formate in **B2**.

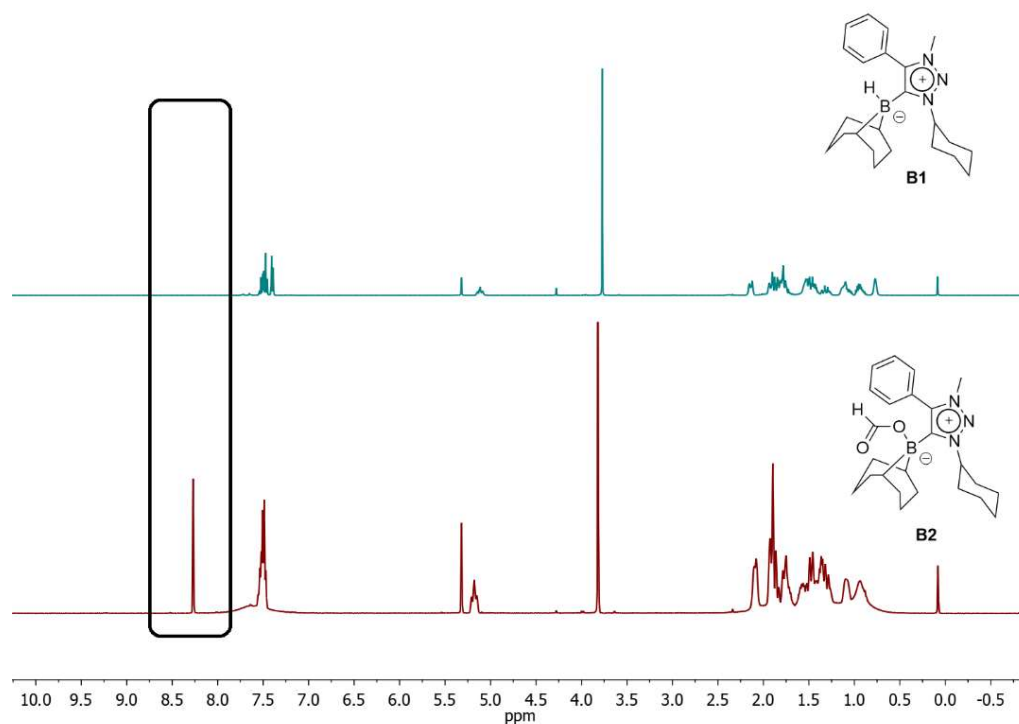


**Figure 3:**  $^1\text{H}$  NMR spectra of **B1** (top) and **B2** (bottom) in  $\text{CD}_2\text{Cl}_2$ .

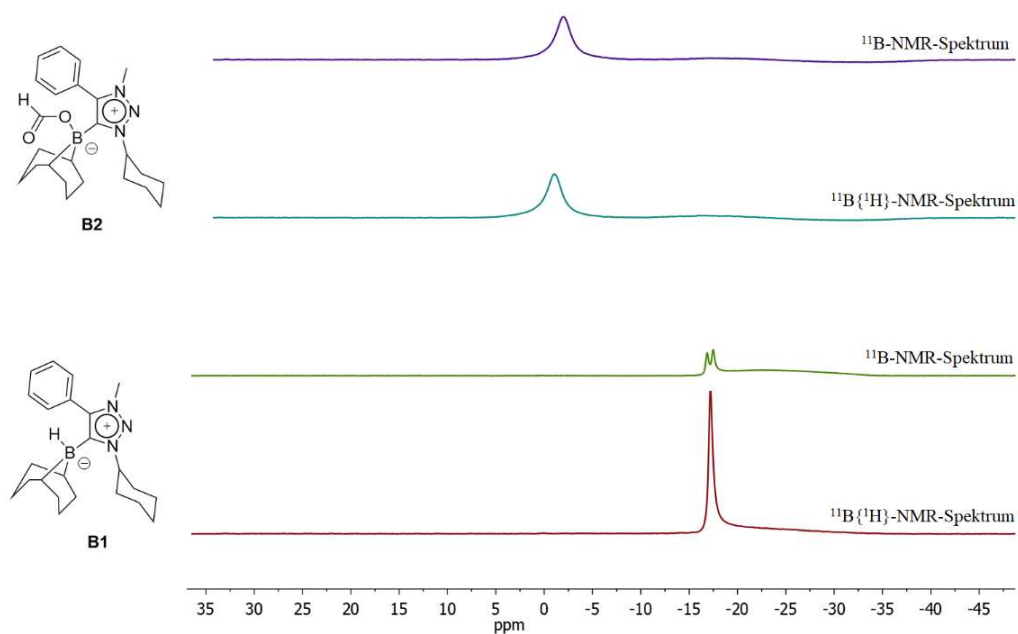


**Figure 4:**  $^{11}\text{B}$  NMR spectra of **B1** (bottom) and **B2** (top) measured in  $\text{CD}_2\text{Cl}_2$ .

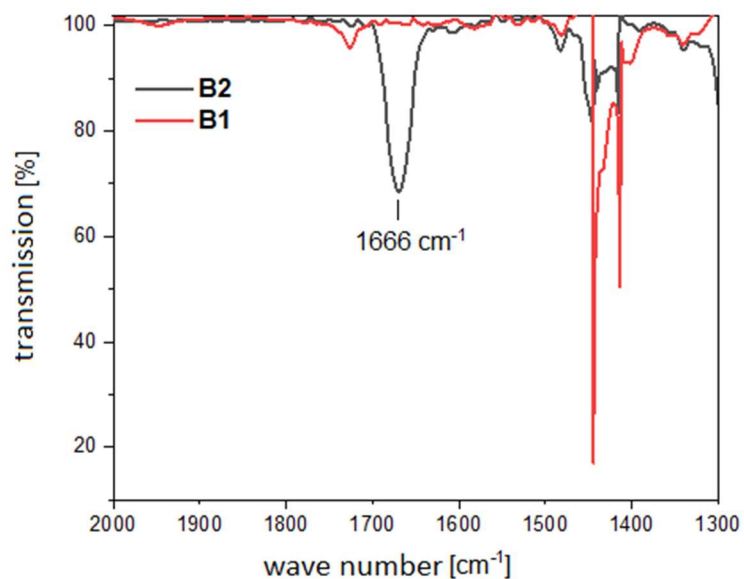


**Figure 5:** IR spectra of **B1** and **B2** in  $\text{CH}_2\text{Cl}_2$ .

The final unequivocal proof for the formation of **B2** came from its single crystal X-ray diffraction analysis (Figure 6). As can be seen from the molecular structure in the crystal, the formate is bound to the boron center. The C1-B1 bond length between the MIC-C and the boron center is 1.644(6) Å, and is in the same range as that observed for **B1**. The O1-C16 and the O2-C16 bond lengths of formate in **B2** are 1.298(5) and 1.208(5) respectively, indicating as expected one shorter and one longer C-O bond. The B1-O1 bond distance is 1.551(6) Å. This structure is also identical in terms of connectivity to the structure obtained from the reaction of **B1** with atmospheric  $\text{CO}_2$  (Figure S4).



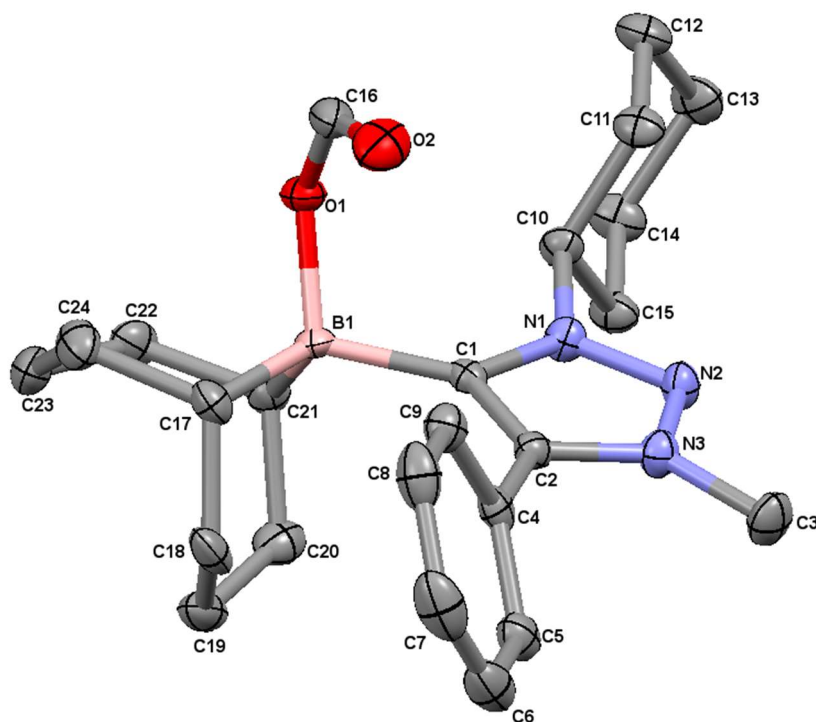


**Figure 6:** ORTEP representation of **B2**. Ellipsoids are drawn at 50 % probability. Solvent molecules and H-atoms have been omitted for clarity. (For selected bond lengths and angles see supporting information Table S3)

In another attempt, CO<sub>2</sub> gas (purity %  $\geq$  99.5) was bubbled through a solution of **B1** in benzene (Scheme 5). In the <sup>1</sup>H spectrum of the product **4** two singlets are observed at 9.31 and 8.47 ppm and these can be assigned to the O-H proton of bicarbonate, and to the C-H proton of the triazolium salt (Figure S15). Additionally, a signal at +18.8 ppm in the <sup>11</sup>B NMR spectrum of **4** confirms the presence of boronic acid. Gratifying, we were also able to obtain single crystals of **4** suitable for X-ray diffraction studies. The data clearly show the formation of an unprecedented triazolium salt of bicarbonate together with boronic acid (Figure 7). In the solid-state molecular structure of **4** all bond lengths within the triazolium moiety are in accordance with values previously reported in the literature.<sup>[21]</sup> Intriguingly, while the reaction of **B1** with atmospheric CO<sub>2</sub> leads eventually to the formation of triazolium formate together with boronic acid (Scheme 3), the reaction of **B1** with “pure” CO<sub>2</sub> dissolved in a solvent leads to the formation of triazolium bicarbonate and boronic acid (Scheme 5). These results thus show the sensitivity of the reactivity of **B1** towards the concentration of CO<sub>2</sub> and/or pH of the solution.

**Scheme 5:** Reaction of **B1** with “pure” CO<sub>2</sub> gas dissolved in benzene.

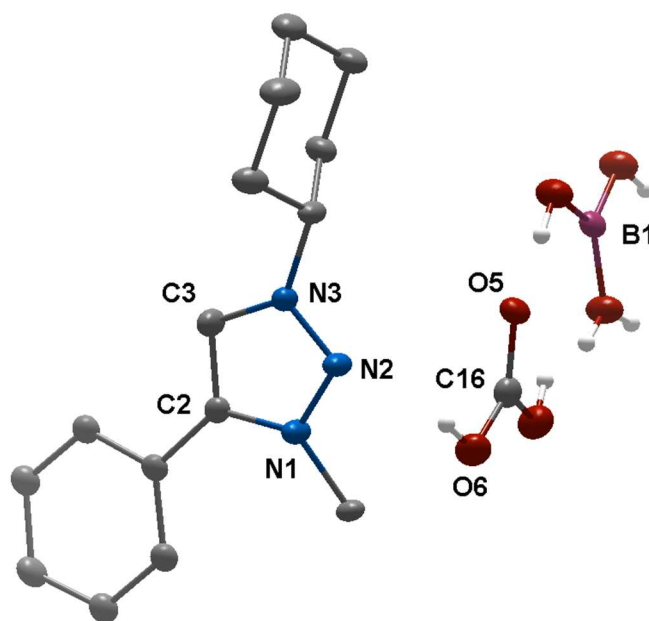
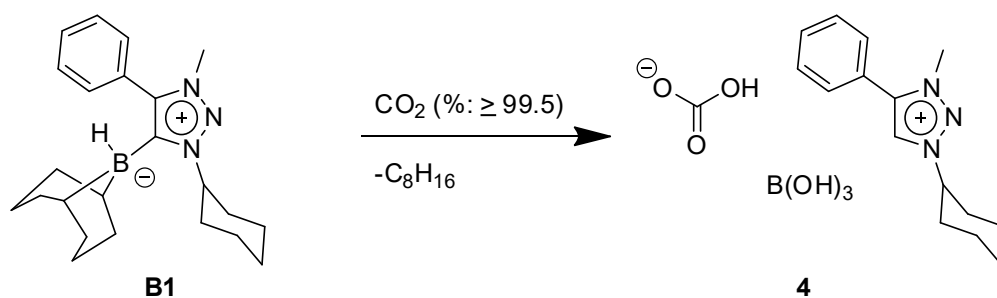
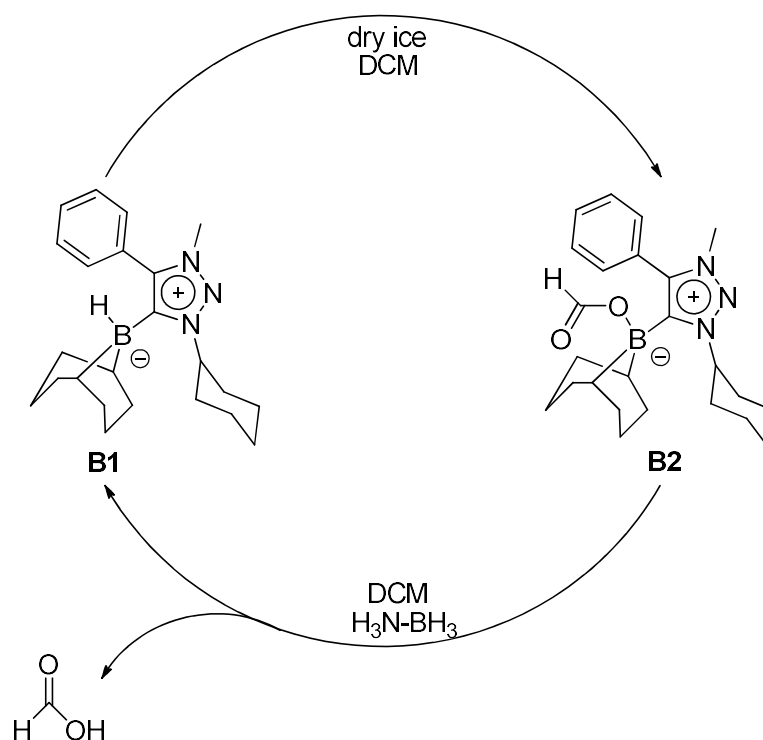


**Figure 7:** ORTEP representation of **4**. Ellipsoids drawn at 50% probability. Solvent molecules and H-atoms omitted for clarity. (For selected bond lengths and angles see supporting information Table S2).

After having all these results in hand, we looked for a way of regenerating **B1** from **B2** coupled with the formation of formic acid. Gratifyingly, as described above, **B1** can be converted to **B2** by using dry ice as a CO<sub>2</sub> source, and **B2** can be converted back to **B1** by using ammonia borane as a proton and a hydride donor to regenerate **B1** through the simultaneous formation of formic acid (Scheme 6, Figure S23 and S24). The formic acid was detected either through a direct GC analysis or by precipitating it as sodium formate (see supporting information).

**Scheme 6:** Conversion of **B1** to **B2** through activation of CO<sub>2</sub>, and the conversion of **B2** back to **B1** by using ammonia borane as a proton and a hydride source.



Summarizing, we have presented here a 1,2,3-triazol-5-ylidene-based mesoionic carbene supported 9-BBN adduct **B1**. The adduct is capable of capturing and reducing CO<sub>2</sub> from air. The greenhouse gas binds to the adduct as formate, which could then be further utilized after cleavage as a formate counter-anion for the generated triazolium salt and boric acid. The reaction of the MIC-borane adduct with CO<sub>2</sub> was found to be strongly dependent on the source of CO<sub>2</sub>, as atmospheric CO<sub>2</sub> lead to the formation of a formate triazolium salt whereas “pure” CO<sub>2</sub> resulted in the formation of a triazolium bicarbonate. By using dry ice, we were able to establish a closed cycle in which the MIC-borane adduct activates and binds CO<sub>2</sub> to form a compound in which the resulting formate is bound to the boron center. That compound could be reacted with ammonia borane to produce formate and regenerate the MIC-borane adduct thus closing the cycle. Besides showcasing the ability of MIC-boranes for CO<sub>2</sub> capture and fixation, our results in general point to the hidden potential of triazolylidene adducts with main group fragments for activating and converting inert small molecules.

#### Acknowledgements

The core facility (BioSupraMol) is gratefully acknowledged.

## References

- [1] D. M. D. Alessandro, B. Smit, J. R. Long, *Angew. Chem. Int. Ed.* **2010**, *49*, 6058–6082.
- [2] M. Aresta, A. Dibenedetto, *Dalton Trans.* **2007**, 2975–2992.
- [3] Z. Jiang, T. Xiao, V. L. Kuznetsov, P. P. Edwards, *Philos. Trans. R. Soc., A* **2010**, *368*, 3343–3364.
- [4] G. A. Olah, A. Goepfert, G. K. S. Prakash, *J. Org. Chem.* **2009**, *74*, 487–498.
- [5] F.-G. Fontaine, M.-A. Courtemanche, M.-A. Légaré, *Chem. - Eur. J.* **2014**, *20*, 2990–2996.
- [6] R. Langer, Y. Diskin-Posner, G. Leitus, L. J. W. Shimon, Y. Ben-David, D. Milstein, *Angew. Chem. Int. Ed.* **2011**, *50*, 9948–9952.
- [7] M. S. Jeletic, M. T. Mock, A. M. Appel, J. C. Linehan, *J. Am. Chem. Soc.* **2013**, *135*, 11533–11536.
- [8] R. Tanaka, M. Yamashita, K. Nozaki, *J. Am. Chem. Soc.* **2009**, *131*, 14168–14169.
- [9] W. Wang, S. Wang, X. Ma, J. Gong, *Chem. Soc. Rev.* **2011**, *40*, 3703–3727.
- [10] S. Chakraborty, J. Zhang, J. A. Krause, H. Guan, *J. Am. Chem. Soc.* **2010**, *132*, 8872–8873.
- [11] C. A. Huff, M. S. Sanford, *J. Am. Chem. Soc.* **2011**, *133*, 18122–18125.
- [12] A. Paparo, J. S. Silvia, C. E. Kefalidis, T. P. Spaniol, L. Maron, J. Okuda, C. C. Cummins, *Angew. Chem. Int. Ed.* **2015**, *54*, 9115–9119.
- [13] C. Das Neves Gomes, E. Blondiaux, P. Thuéry, T. Cantat, *Chem. - Eur. J.* **2014**, *20*, 7098–7106.
- [14] M.-A. Courtemanche, M.-A. Légaré, L. Maron, F.-G. Fontaine, *J. Am. Chem. Soc.* **2013**, *135*, 9326–9329.
- [15] T. Wang, D. W. Stephan, *Chem. - Eur. J.* **2014**, *20*, 3036–3039.
- [16] S. N. Riduan, Y. Zhang, J. Y. Ying, *Angew. Chem. Int. Ed.* **2009**, *48*, 3322–3325.
- [17] S. C. Sau, R. Bhattacharjee, P. K. Vardhanapu, G. Vijaykumar, A. Datta, S. K. Mandal, *Angew. Chem. Int. Ed.* **2016**, *55*, 15147–15151.
- [18] T. Wang, D. W. Stephan, *Chem. Commun.* **2014**, *50*, 7007–7010.
- [19] I. Knopf, C. C. Cummins, *Organometallics* **2015**, *34*, 1601–1603.
- [20] S. Chandra Sau, R. Bhattacharjee, P. K. Hota, P. K. Vardhanapu, G. Vijaykumar, R. Govindarajan, A. Datta, S. K. Mandal, *Chem. Sci.* **2019**, *10*, 1879–1884.
- [21] N. Khan, Y. Ingen, T. Boruah, A. McLauchlan, T. Wirth, R. Melen, *Chem. Sci.* **2023**, *14*, 13661–13695.
- [22] J. Fan, A. Koh, C. Wu, M. Su, C. So, *Nat. Commun.* **2024**, *15*, 3052.
- [23] A. Stoy, J. Böhnke, J. Jiménez-Halla, R. Dewhurst, T. Thiess, H. Braunschweig, *Angew. Chem. Int. Ed.* **2018**, *57*, 5947.
- [24] J. Fan, J. Mah, M. Yang, M. Su, C. So, *J. Am. Chem. Soc.* **2021**, *143*, 4993–5002.
- [25] D. Wu, L. Kong, Y. Li, R. Ganguly, R. Kinjo, *Nat. Commun.* **2015**, *6*, 7340.
- [26] D. Wu, R. Wang, Y. Li, R. Ganguly, H. Hirao, R. Kinjo, *Chem* **2017**, *3*, 134–151.

- [27] K. Wentz, A. Molino, L. Freeman, D. Dickie, D. Wilson, R. Gilliard, *J. Am. Chem. Soc.* **2022**, *144*, 16276-16281.
- [28] X. Chen, Y. Yang, H. Wang, Z. Mo, *J. Am. Chem. Soc.* **2023**, *145*, 7011-7020.
- [29] R. Maity, B. Sarkar, *JACS Au* **2022**, *2*, 22–57.
- [30] D. Schweinfurth, L. Hettmanczyk, L. Suntrup, B. Sarkar, *Z. Anorg. Allg. Chem.* **2017**, *643*, 554–584.
- [31] Á. Vivancos, C. Segarra, M. Albrecht, *Chem. Rev.* **2018**, *118*, 9493-9586.
- [32] G. Guisado-Barrios, M. Soleilhavoup, G. Bertrand *Acc. Chem. Res.* **2018**, *51*, 3236-3244.
- [33] T. Bens, R. Walter, J. Beerhues, M. Schmitt, I. Krossing, B. Sarkar, *Chem. Eur. J.* **2023**, *29*, e202301205.
- [34] B. Wittwer, N. Dickmann, S. Berg, D. Leitner, L. Tesi, David Hunger, R. Gratzl, J. Slageren, N. Neuman, D. Munz, S. Hohloch, *Chem. Commun.* **2022**, *58*, 6096-6099.
- [35] L. Suntrup, S. Klenk, J. Klein, S. Sobottka, B. Sarkar, *Inorg. Chem.* **2017**, *56*, 5771-5783.
- [36] J. Stubbe, S. Suhr, J. Beerhues, M. Nößler, B. Sarkar, *Chem. Sci.* **2021**, *12*, 3170-3178.
- [37] L. Freitas, P. Eisenberger, C. Crudden, *Organometallics* **2013**, *32*, 6635-6638.
- [38] P. Eisenberger, B. Bestvater, E. Keske, C. Crudden, *Angew. Chem. Int. Ed.* **2015**, *54*, 2467-2471.
- [39] F. Stein, M. Kirsch, J. Beerhues, U. Albold, B. Sarkar, *Eur. J. Inorg. Chem.* **2021**, *24*, 2417-2424.